

Violations of Bell's inequality for Gaussian states with homodyne detection and nonlinear interactions

M. Paternostro,¹ H. Jeong,^{2,3} and T. C. Ralph³

¹*School of Mathematics and Physics, Queen's University, Belfast BT7 1NN, United Kingdom*

²*Center for Subwavelength Optics and Department of Physics and Astronomy, Seoul National University, Seoul 151-742, Korea*

³*Center for Quantum Computer Technology, Department of Physics, University of Queensland, St. Lucia, Queensland 4072, Australia*

(Received 20 November 2008; published 5 January 2009)

We show that homodyne measurements can be used to demonstrate violations of Bell's inequality with Gaussian states, when the local rotations used for these types of tests are implemented using nonlinear unitary operations. We reveal that the local structure of the Gaussian state under scrutiny is crucial in the performance of the test. The effects of finite detection efficiency are thoroughly studied and shown to only mildly affect the revelation of Bell violations. We speculate that our approach may be extended to other applications such as entanglement distillation where local operations are necessary elements besides quantum entanglement.

DOI: [10.1103/PhysRevA.79.012101](https://doi.org/10.1103/PhysRevA.79.012101)

PACS number(s): 03.65.Ud, 03.67.Mn, 42.50.Dv

I. INTRODUCTION

Violation of Bell's inequality [1,2], which means failure of local realism, is perhaps the most profound yet controversial feature of quantum mechanics. It was Einstein, Podolsky, and Rosen (EPR)'s work which challenged the completeness of quantum mechanics as a theory [3]. Although the original formulation of EPR's paradox involved the state of a bipartite system having a continuous spectrum, Bohm's version of the problem [4] and the seminal work by Bell [1,2] moved the debate toward its discrete version, which quickly became the paradigm in the physics community.

The proved experimental handiness of continuous variable (CV) systems, epitomized by proposals and realizations of schemes for quantum teleportation [5], among other examples, has redirected considerable interest toward the investigation of Bell's inequality with these states. It has been known since Bell that the original EPR state allows a realistic description in terms of the canonically conjugated variables of position and momentum because its Gaussian Wigner function can be used as a classical probability distribution for a hidden variable model [2]. Later, however, it has been proven that a two-mode squeezed vacuum state, whose Wigner function is a Gaussian, can violate Bell's inequality, although nonoptimal, in the joint measurement of phase-space displaced parity operator [6]. The loophole here is that the inclusion of photon counting measurements (necessary for parity determination) negates a realistic interpretation of the Wigner function [7]. This result has triggered extensive investigation on the interplay between measurements and the Gaussian character of CV states in Bell's inequality tests. It has been found that non-Gaussian CV entangled states can be used to demonstrate violations of Bell's inequality by means of Gaussian measurements (i.e., measurements that preserve the Gaussian nature of a state, such as homodyne detection) [8]. It has also been shown that a *nondeterministic* Bell's inequality test can be devised using Gaussian CV states to show Bell violations when non-Gaussian conditioning measurements are combined with homodyne measurements [9]. However, in virtue of Bell's argument for a realistic description of an EPR state, it is well known that Bell's

inequality tests, in which both states and measurements are Gaussian, are destined to the satisfaction of Bell's inequality [2]. More practically, this "no-go" result seems paired with the impossibility of entanglement distillation for Gaussian states under Gaussian-preserving operations [10], which in turn limits the implementation of efficient quantum repeaters for Gaussian states [11].

In this paper, we describe a different angle on the aforementioned problems. We examine Clauser-Horne-Shimony-Holt (CHSH)'s version of Bell's inequality [12] and show its violation by Gaussian states subjected to nonlinear local unitary operations and homodyne measurements. In order to efficiently illustrate our findings, which we describe with respect to routinely generated entangled Gaussian states, it is convenient to first address a situation where the local operations required for our Bell's inequality test are treated as ideal single qubit rotations [13] for coherent-state qubits [14,15]. We then present physical transformations [14] which are able to reproduce the core features of the idealized case (cf. Fig. 1). In both ideal and physical cases, a considerable (although nonoptimal) degree of violation of the Bell-CHSH test is found, resilient to imperfections at the detection stage. Our study shows that the local unitary operations, the importance of which has not previously been carefully examined, may play a key role in utilizing Gaussian states for Bell's inequality tests and, possibly, other applications such as entanglement distillation. Our protocol is shown to be quite resilient to spoiling effects such as nonzero temperatures and low detection efficiency. We also stress that our scheme makes use of Gaussian squeezed states, which are resources routinely employed in all-optical experiments dealing with continuous variables. This distinguishes our proposal from the case of entangled coherent states being used for Bell's inequality tests (such as in Ref. [13]), which are non-Gaussian and more demanding to produce.

The remainder of this paper is organized as follows. In Sec. II we describe the formal approach to our Bell's inequality test. We introduce the Gaussian states we probe and the class of nonlinear unitary operations we consider. This is achieved by first studying a sort of idealized case and then moving to the real physical situation. We show that Bell's

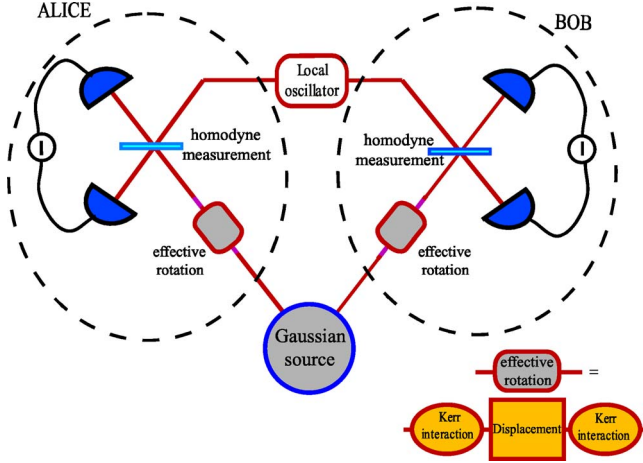


FIG. 1. (Color online) Schematic of a Bell-CHSH inequality test with Gaussian states and homodyne measurements. A quantum correlated two-mode Gaussian state is produced at a source and distributed to Alice and Bob who perform local effective rotations and homodyne measurements. The effective rotations are physically implemented by cascading Kerr-type nonlinearities and phase-space displacement operations, as shown in the inset. The Gaussian state produced by the source can be either a two-mode squeezed state or the state resulting from the superposition, at a 50:50 beam splitter, of vacuum and a single-mode squeezed state.

inequality can be violated by Gaussian states with homodyne measurements using the specific class of operations. In Sec. III we study the effects of detection inefficiencies and show that they can be counteracted by increasing the squeezing of the initial resource. This very same strategy can be used in order to cope with a mixedness initial state instead of a pure, ideal resource. This is consistent with a previous result [16] using entangled thermal states [17], where the same effects could be achieved by increasing the distance between the component thermal states [16]. Section IV shows that the required level of squeezing to show Bell violations can be considerably reduced when another class of experimentally relevant Gaussian states are used. Finally, in Sec. V we summarize our results and discuss their physical implications.

II. TEST FOR BELL'S INEQUALITY

In Ref. [13], it was shown that a superposition of two coherent states, $|c_+\rangle = N_+(|\alpha\rangle + |-\alpha\rangle)$ with the normalization factor N_+ and coherent states $|\pm\alpha\rangle$ of amplitudes $\pm\alpha$, when divided at a beam splitter, violates Bell-CHSH inequality using homodyne measurements and nonlinear interactions. One can show that the fidelity \mathcal{F} between a coherent-state superposition $|c_+\rangle$ and a single-mode squeezed state is very high when α is relatively small (e.g., $\mathcal{F} \geq 0.99$ for $\alpha < 0.75$). This motivates us to first investigate violation of Bell's inequality for single-mode squeezed states divided at a beam splitter. We shall later study another set of Gaussian states which outperform the results for this case.

Let us suppose that two parties, Alice and Bob, share an entangled state generated using a single-mode squeezed vacuum and a 50:50 beam splitter [18]. Analytically, the state

can be described by the following Gaussian-weighted continuous superposition of coherent states [19]

$$|\xi\rangle_{AB} = \mathcal{N} \int d^2\alpha \mathcal{G}(r, \alpha) \left| \frac{\alpha}{\sqrt{2}}, \frac{\alpha}{\sqrt{2}} \right\rangle_{AB}, \quad (1)$$

where $\mathcal{G}(r, \alpha) = \exp[-(1 - \tanh r)\alpha^2 / (2 \tanh r)]$, r is the squeezing parameter, $\alpha \in \mathbb{R}$, and $\mathcal{N} = 1/\sqrt{2\pi \sinh r}$ is the normalization factor. The class of nonlinear transformations we consider can be understood as an approximation of the following rotations performed in the bidimensional space spanned by the generic coherent state $\{|\pm\beta\rangle\}$ ($\beta \in \mathbb{C}$) [13],

$$\hat{R}_j(\theta)|\beta\rangle_j \rightarrow \sin(2\theta_j)|\beta\rangle_j + \cos(2\theta_j)|-\beta\rangle_j,$$

$$\hat{R}_j(\theta)|-\beta\rangle_j \rightarrow \cos(2\theta_j)|\beta\rangle_j - \sin(2\theta_j)|-\beta\rangle_j, \quad (2)$$

where θ_j is the effective ‘‘angle’’ of such idealized rotations and $j=A, B$ labels Alice’s or Bob’s site. It should be noted that the ‘‘idealized’’ transformation described in Eq. (2) is *not* unitary (approximately unitary when β is large) so that it cannot be performed deterministically. The actual physical local transformation using nonlinear interactions will be considered later in this section.

After the application of the local operations (2) to their respective mode, Alice and Bob perform bilocal homodyne measurements, which result in the joint probability amplitude function

$$C_{id}(\theta_A, \theta_B, x, y) \propto \langle x, y | \hat{R}_A(\theta_A) \hat{R}_B(\theta_B) | \xi \rangle_{AB} \quad (3)$$

with $|x\rangle$ ($|y\rangle$) the in-phase quadrature eigenstate of Alice’s (Bob’s) mode. A sketch of the thought experiment is presented in Fig. 1. In order to test the CHSH version of Bell’s inequality, we need to construct a set of bounded dichotomic observables, which we do by assigning value +1 to a homodyne measurement’s outcome larger than 0, and -1 otherwise [8]. With this, a joint probability of outcomes can be calculated as

$$P_{kl}(\theta_A, \theta_B) = \int_{k_i}^{k_s} dx \int_{l_i}^{l_s} dy |C_{id}(\theta_A, \theta_B, x, y)|^2, \quad (4)$$

where the subscripts $k, l = \pm$ correspond to Alice’s and Bob’s assigned measurement outcomes ± 1 and the integration limits are such that $+_s = \infty$, $+_i = -_s = 0$, and $-_i = -\infty$. We can now calculate the Bell-CHSH function, $B(\theta_A, \theta_B, \theta'_A, \theta'_B) = C(\theta_A, \theta_B) + C(\theta'_A, \theta'_B) + C(\theta_A, \theta'_B) - C(\theta'_A, \theta_B)$, where we have introduced the correlation function

$$C(\theta_A, \theta_B) = \sum_{k=\pm} P_{kk}(\theta_A, \theta_B) - \sum_{k \neq l = \pm} P_{kl}(\theta_A, \theta_B). \quad (5)$$

According to local-realistic theories, the Bell-CHSH inequality $|B(\theta_A, \theta_B, \theta'_A, \theta'_B)| \leq 2$ holds. Quantitatively, we have found that

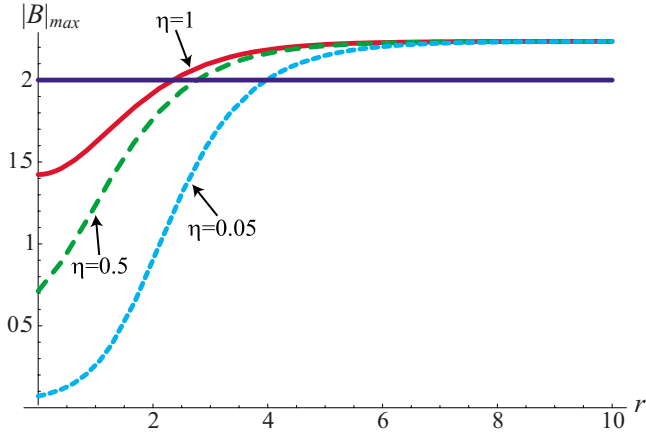


FIG. 2. (Color online) Bell test for ideal rotations. The Bell-CHSH function is plotted against the squeezing parameter r for three values of the detection efficiency η . We show the case corresponding to ideal homodyne detection (solid line), $\eta=0.5$ (dashed line), and $\eta=0.05$ (dotted line). The horizontal line shows the bound for local realistic theories.

$$C_{id}(\theta_A, \theta_B, r) = \frac{2 \arctan(\sinh r) \cos(4\theta_A) \cos(4\theta_B)}{\pi \left(1 + \sum_{j \neq k} \sin(4\theta_j) \left[\frac{\sin(4\theta_k)}{2} + \sinh r \right] \right)}, \quad (6)$$

with $j, k=A, B$, and the subscript id is used in order to remind one of the idealized version of local operations being used. The behavior of the numerically optimized Bell-CHSH function corresponding to Eq. (6) is shown by the solid curve in Fig. 2, which demonstrates that a local realistic description of $|\xi\rangle_{AB}$ is impossible as the squeezing parameter for the initial single-mode state surpasses ~ 2.1 . The degree of violation of the Bell-CHSH inequality then reaches a maximum of ~ 2.23 , robustly against r .

Now that we have gained a quantitative picture of the behavior of the Bell function under the class of formal operations and Gaussian measurements considered in our work, it is time to provide a physically effective description of each rotation $\hat{R}_j(\theta_j)$. Such physical implementation stems from the observation made in Ref. [13] that Eqs. (2) can be approximated by a combination of single-mode Kerr interaction $\hat{U}_{\text{Kerr}} = e^{-i\hat{H}_{\text{Kerr}}t}$ with $\hat{H}_{\text{Kerr}} = \hbar\Omega(\hat{a}^\dagger\hat{a})^2$ (Ω being the strength of the nonlinear coupling) and displacement of amplitude $\varphi \in \mathbb{C}$, $\hat{D}(\varphi) = e^{\varphi\hat{a}^\dagger - \varphi^*\hat{a}}$. Here \hat{a} (\hat{a}^\dagger) is the annihilation (creation) operator of a field mode. A single-mode Kerr interaction may be implemented, for example, by nonlinear crystals [20,21] while the displacement can be easily performed via a beam splitter with high transmittivity and a local oscillator.

In detail, the evolution induced by the effective rotations $\hat{V}_j(\theta_j) = \hat{U}_{\text{Kerr}}\hat{D}(i\theta_j/d)\hat{U}_{\text{Kerr}}$ on input coherent states $|\pm\beta\rangle_j$ is given by the following expressions ($\beta = \beta_r + i\beta_i$ and $d \in \mathbb{R}$ determines the amplitude of the displacement) [13]:

$$\begin{aligned} \hat{V}_j(\theta_j)|\beta\rangle_j &= \frac{1}{2} \left\{ e^{i\theta_j\beta_r/d} \left(\left| \beta + \frac{i\theta_j}{d} \right\rangle_j + i \left| -\beta - \frac{i\theta_j}{d} \right\rangle_j \right) \right. \\ &\quad \left. + i e^{-i\theta_j\beta_r/d} \left(\left| -\beta + \frac{i\theta_j}{d} \right\rangle_j + i \left| \beta - \frac{i\theta_j}{d} \right\rangle_j \right) \right\}, \\ \hat{V}_j(\theta_j)|-\beta\rangle_j &= \frac{1}{2} \left\{ i e^{i\theta_j\beta_r/d} \left(\left| \beta + \frac{i\theta_j}{d} \right\rangle_j + i \left| -\beta - \frac{i\theta_j}{d} \right\rangle_j \right) \right. \\ &\quad \left. + e^{-i\theta_j\beta_r/d} \left(\left| -\beta + \frac{i\theta_j}{d} \right\rangle_j + i \left| \beta - \frac{i\theta_j}{d} \right\rangle_j \right) \right\}. \end{aligned} \quad (7)$$

Note that $\hat{V}_j(\theta_j)$ is unitary while $\hat{R}_j(\theta_j)$ is not strictly a unitary operation. The physical operation $\hat{V}_j(\theta_j)$ is a good approximation of the ideal operation $\hat{R}_j(\theta_j)$ when the amplitudes of coherent states on which the operation is acted upon are large. As seen in Eq. (1), our squeezed state can be expanded in terms of coherent states with a Gaussian weight factor as a function of the coherent amplitude. When the squeezing r is large, contributions of coherent states of small amplitudes will become arbitrarily small. This implies that as the squeezing r becomes large, the results of the Bell-CHSH inequality violation using the ideal rotation $\hat{R}_j(\theta_j)$ should be closer to the results using the physical rotation $\hat{V}_j(\theta_j)$.

We then adjust our notation and indicate with $C_{ef}(\theta_A, \theta_B, x, y) = |\langle x, y | \hat{V}_A(\theta_A) \hat{V}_B(\theta_B) | \xi \rangle_{AB}|^2$ the probability of measuring the values x and y of the quadrature variables at the homodyne detectors. The subscript clearly states that this is the function associated with the use of physical effective rotations. Quantitatively, C_{ef} is easily found using the projection of a coherent state onto a position quadrature eigenstate $|x\rangle$, which is given by $\langle x | \beta \rangle = \pi^{-1/4} e^{\sqrt{2}i\beta_r x - 1/2(x - \sqrt{2}\beta_r)^2 - i\beta_r\beta_i}$ [18]. We eventually obtain

$$\begin{aligned} |C_{ef}(\theta_A, \theta_B, x, y)|^2 &= \frac{1}{\pi} e^{-r - e^{-r} \cosh r(x^2 + y^2)} \left[e^{xye^{-2r}} \sin\left(\frac{\sqrt{2}(y\theta_A + x\theta_B)}{d}\right) \right. \\ &\quad \left. + e^{xy} \cos\left(\frac{\sqrt{2}(y\theta_A - x\theta_B)}{d}\right) \right]. \end{aligned} \quad (8)$$

We are now in a position to build up the Bell-CHSH function for our Bell's inequality test in such a physically effective case. Unfortunately, producing an analytic result is rather demanding due to the semi-infinite range of integrations over the quadrature variables x and y , which also enter into the trigonometric functions in Eq. (8), required in order to gather the joint probabilities $P_{kl}(\theta_A, \theta_B)$. We have therefore performed the Bell's inequality test by numerically evaluating the Bell-CHSH function for a set value of d and by scanning the squeezing parameter r . The results are shown by the top-most curve in Fig. 3, where violation of local realistic theories starting from $r \gtrsim 2.1$ is observed, which is in full agreement with the ideal-rotation case. Also, the degree of violation is consistent between the two cases, $|B|_{\text{max}}$ being 2.229 at $r=3.3$. Although the reproduction of the behavior

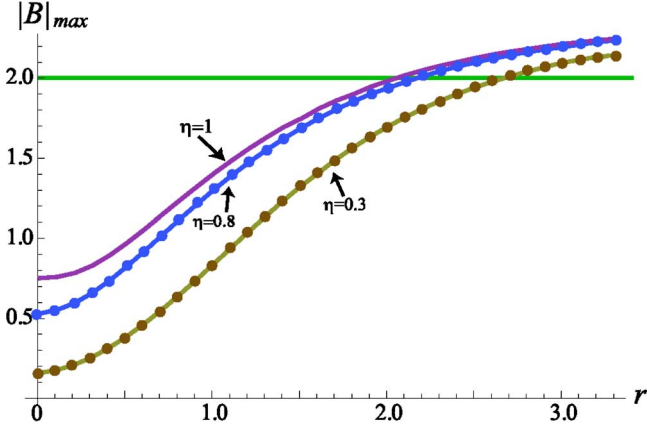


FIG. 3. (Color online) The numerically optimized Bell function is plotted against the squeezing parameter r for the case of physical effective rotations and three values of detection efficiency. The horizontal line shows the bound for local realistic theories. The actual value of d is irrelevant in this figure. The solid line with $\eta=1$ embodies the ideal-detector case with the other two cases of $\eta=0.8$ and $\eta=0.3$.

for large r is computationally demanding, it is possible to perform a qualitative comparison between the ideal and effective cases by looking at the corresponding joint probability functions $|C_{id}(\theta_A, \theta_B, x, y)|^2$ and Eq. (8), evaluated at the angles corresponding to the (numerically optimized) associated Bell-CHSH function. This is done in Fig. 4, where the clear similarity of the two probability functions ensures the closeness of the value of the corresponding Bell-CHSH functions.

III. ROBUSTNESS TO IMPERFECTIONS

Although homodyne detectors have rather high efficiencies, the violation of the Bell-CHSH inequality by $|\xi\rangle_{AB}$ is far from $2\sqrt{2}$, the maximum given by Tsirelson's bound [22]. One might thus wonder whether even mild detection inefficiencies are sufficient to wash out the Bell-CHSH inequality violation unveiled in Fig. 3. An important issue to address is thus given by the effects of detection inefficiencies. As done before, we first gain an idea of the expected behavior by studying the idealized picture.

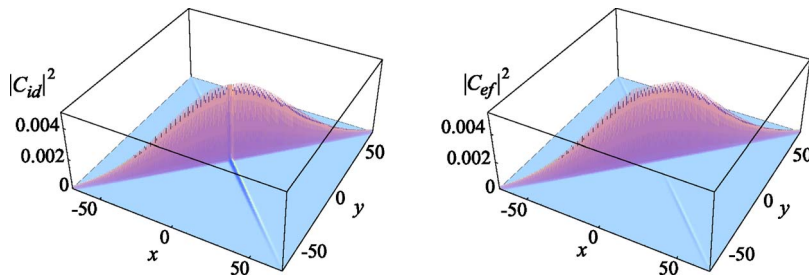


FIG. 4. (Color online) We compare the behavior of the joint-probability functions $|C_{id}(\theta_A, \theta_B, x, y)|^2$ and $|C_{ef}(\theta_A, \theta_B, x, y)|^2$ against the quadrature variables x and y for $r=4$. The angles $\theta_{A,B}$ are those maximizing the corresponding Bell-CHSH function. We thus have $\theta_A=0.061$ and $\theta_B=0.182$ ($\theta_A=-0.009$ and $\theta_B=0.004$) for the leftmost (rightmost) plot. Moreover, $\iint dx dy |C_{ef}(\theta_A, \theta_B, x, y)|^2 \simeq \iint dx dy |C_{id}(\theta_A, \theta_B, x, y)|^2$, regardless of the domain of integration.

In order to quantitatively assess this point, we have modeled the imperfect homodyne detector onto which mode $j=A, B$ impinges as the cascade of a beam splitter of transmissivity η , mixing mode j to an ancillary vacuum mode a_j , and a perfect homodyner. We are not interested in the state of the ancillae, which are discarded by tracing them out of the overall state, so that $|C_{id}(\theta_A, \theta_B, x, y)|^2$ is changed into $\langle x, y | \text{Tr}_{a_A a_B} \psi(\theta_A, \theta_B) | x, y \rangle$ with

$$\begin{aligned} \psi(\theta_A, \theta_B) &= \hat{B}_{Aa_A}(\eta) \hat{B}_{Ba_B}(\eta) \hat{R}_A(\theta_A) \hat{R}_B(\theta_B) |\xi\rangle_{AB} \langle \xi| \\ &\otimes |00\rangle_{a_A a_B} \langle 00| \hat{R}_A^\dagger(\theta_A) \hat{R}_B^\dagger(\theta_B) \hat{B}_{Aa_A}^\dagger(\eta) \hat{B}_{Ba_B}^\dagger(\eta), \end{aligned} \quad (9)$$

where the beam splitter operation between modes j and the corresponding ancilla a_j is defined as $\hat{B}_{ja_j}(\zeta) = \exp[\zeta/2(\hat{a}_j^\dagger \hat{b}_{a_j} - \hat{a}_j \hat{b}_{a_j}^\dagger)]$ with $\cos \zeta = \sqrt{\eta}$ and \hat{b}_{a_j} being the annihilation operator of a_j [23]. The remaining procedure for the construction of the appropriate Bell-CHSH function remains as described above. The final form of the correlation function, which now depends on the efficiency as well, is obtained from Eq. (6) by simply replacing $\arctan(\sinh r) \rightarrow \arctan(\frac{\eta e^r \sinh r}{\sqrt{1+2\eta e^r \sinh r}})$. The behavior of the associated Bell function is shown, for two values of η , in Fig. 2. We observe a rather striking robustness of the Bell function with respect to the homodyners' inefficiency: Even severely inefficient homodyne detectors would be able to unveil Bell-CHSH inequality violations with a state which is initially squeezed enough. By simply increasing the squeezing of the input state, one can compensate the effects of detection inefficiencies. Although for small values of η , the required squeezing factor becomes prohibitively large, the trend revealed by the ideal case leaves quite a few hopes for the physical effective one as well. In fact, such robustness persists when the local operations (7) are used, as shown in Fig. 3 for $\eta=0.8$ and 0.3 (chosen for easiness of representation). The squeezing threshold at which the Bell's inequality test starts to be violated increases only quite slowly as the quality of the homodyne detectors is degraded. In passing, we should stress that the beam-splitter model used for the description of an inefficient homodyne detector can be used in order to describe the influences of external zero-temperature reservoirs coupled to the correlated two-mode state we are studying.

Thus, similar conclusions regarding the resilience of the Bell-CHSH function to losses induced by a low-temperature environment can be drawn.

We complete our study about the effects of imperfections by investigating the case in which we start with a mixed resource. This is practically quite relevant, given the fact that, experimentally, a single-mode squeezed thermal state is in general produced instead of a pure single-mode squeezed vacuum state. This is formally accounted for by considering the resource state

$$\rho_{AB}^{st} = \int d^2\alpha \mathcal{T}(\bar{n}, \alpha) \hat{S}_A(r) \left| \frac{\alpha}{\sqrt{2}}, \frac{\alpha}{\sqrt{2}} \right\rangle_{AB} \left\langle \frac{\alpha}{\sqrt{2}}, \frac{\alpha}{\sqrt{2}} \right| \hat{S}_A^\dagger(r), \quad (10)$$

where $\mathcal{T}(\bar{n}, \alpha) = e^{-|\alpha-d|^2/\bar{n}} / \pi\bar{n}$ ($\alpha = \alpha_r + i\alpha_i$) is the Glauber-Sudarshan function of a single-mode state at thermal equilibrium with mean photon number \bar{n} and displaced, in phase space, by $d \in \mathbb{R}$ [18], while $\hat{S}_A(r) = e^{r/2(\hat{a}_A^\dagger - \hat{a}_A)^2}$ is the mode- A squeezing operator. Equation (10) results from superimposing at a 50:50 beam splitter a squeezed displaced thermal state of mode A and the vacuum state of mode B . It is straightforward to find that Eq. (10) can be written as $\rho_{AB}^{st} = \int d^2\alpha \tilde{\mathcal{T}}(r, V, \alpha) |\alpha/\sqrt{2}, \alpha/\sqrt{2}\rangle_{AB} \langle \alpha/\sqrt{2}, \alpha/\sqrt{2}|$ with $V = 2\bar{n} + 1$ and

$$\tilde{\mathcal{T}}(r, V, \alpha) = \frac{2e^{-2\alpha_r^2/(e^{2r}V-1) - [(2\alpha_r - d)^2/(e^{-2r}V-1)]}}{\pi\sqrt{V^2 + 1 - 2V \cosh(2r)}}. \quad (11)$$

This state is then locally rotated and projected onto quadrature eigenstates by means of homodyne measurements. Once more, for clarity of our arguments, we refer to the case of ideal rotations. The use of our formal procedure applied so far lead to the correlation function

$$\begin{aligned} C_{st}(\theta_A, \theta_B, r) &= \frac{2 \arctan\left(\frac{e^r - Ve^{-r}}{2\sqrt{V}}\right) \cos(4\theta_A) \cos(4\theta_B)}{\pi \left[1 + \frac{\sin(4\theta_A) \sin(4\theta_B)}{V} + \frac{2\sin(4\theta_A) + \sin(4\theta_B)}{\sqrt{V^2 + 1 + 2V \cosh(2r)}} \right]}. \end{aligned} \quad (12)$$

Clearly, $C_{st} \equiv C_{id}$ when $V=1$, i.e., when a pure state is generated. With this expression, one can easily build up the Bell-CHSH function and test its behavior against the thermal parameter V and, as usual, the squeezing. The results are shown in Fig. 5, where it is shown that it is enough to consider a slightly more squeezed initial resource in order to counteract any thermal effect. The same conclusions are reached by using the set of nonlinear unitary transformations $\hat{V}_j(\theta_j)$, although the analysis is largely numerical and more involved.

IV. IMPROVEMENT USING TWO-MODE SQUEEZED STATES

The required level of squeezing, e.g., $r \geq 2$ for $\eta \geq 0.8$, revealed in Figs. 2 and 3 to demonstrate Bell-CHSH inequality

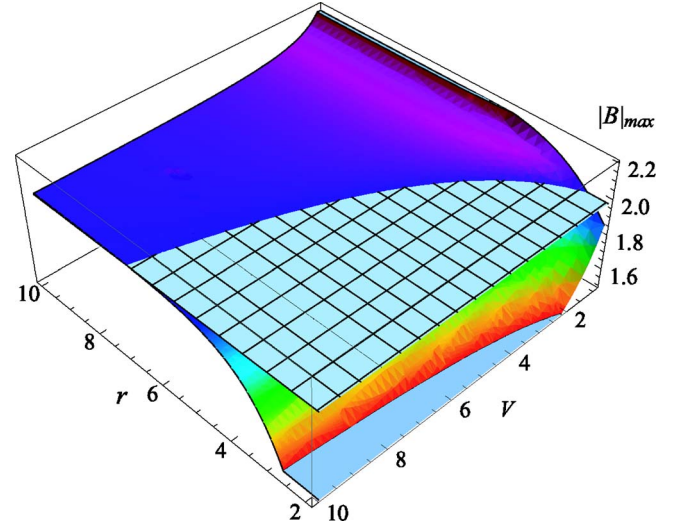


FIG. 5. (Color online) Bell-CHSH test for an input squeezed thermal state superimposed to vacuum at a 50:50 beam splitter. The Bell-CHSH function is plotted against r and $V = 2\bar{n} + 1$, i.e., the thermal variance of the state. The horizontal plane shows the bound for local realistic theories.

violations is experimentally difficult to achieve using current technology. In this section, we show that this requirement can be radically reduced by using another class of Gaussian states. So far, we have investigated the Bell's inequality test under nonlinear operations using the paradigmatic source given by state $|\xi\rangle_{AB}$. However, the behavior of a Bell-CHSH function strongly depends on intrinsic properties of the tested quantum correlated state. In fact, this can be seen as the “dual” of the well-known fact that the same bipartite entangled state behaves differently, in terms of Bell inequality tests, under different sets of local operations. Here, we are interested in finding out whether another realistic Gaussian resource is conceivable for the violation of our Bell-CHSH inequality when smaller values of r are taken. Our starting point is the observation [24,25]

$$\hat{B}_{AB} \left(\frac{\pi}{2} \right) \hat{S}_A(r) |0, 0\rangle_{AB} = \hat{S}_A \left(\frac{r}{2} \right) \hat{S}_B \left(\frac{r}{2} \right) \hat{S}_{AB} \left(\frac{r}{2} \right) |00\rangle_{AB}, \quad (13)$$

where we have used the single-mode squeezing operator $\hat{S}_j(r) = \exp[\frac{r}{2}(\hat{a}_j^2 - \hat{a}_j^{\dagger 2})]$ ($j=A, B$) and its two-mode version $\hat{S}_{AB}(r) = \exp[r(\hat{a}_A^\dagger \hat{a}_B^\dagger - \hat{a}_A \hat{a}_B)]$. Therefore, our resource $|\xi\rangle_{AB}$ is formally equivalent to a two-mode squeezed state that is also subjected to additional local squeezing operation. These latter are unable to change the nonlocal content of the state being used and could well be regarded as a prestage of the local actions (comprising nonlinear rotations and homodyne measurements) performed at Alice's and Bob's site, respectively. We now remove them from the overall setup for Bell's inequality tests by considering, instead of Eq. (1), the standard two-mode squeezed vacuum [26]

$$|\xi'\rangle = \mathcal{M} \int d^2\beta G'(r, \beta) |\beta, \beta^*\rangle \quad (14)$$

with weight function [27]

$$G'(r, \beta) = \exp\left(-\frac{1 - \tanh r |\beta|^2}{\tanh r}\right) \quad (15)$$

and normalization factor $\mathcal{M} = (\pi \sinh r)^{-1}$. The adaptation of the formal procedure described in our work to the use of this Gaussian resource is quite straightforward. For the simple case of ideal local rotations, the correlation function for joint outcomes at Alice's and Bob's site is identical to Eq. (6) with the replacement $r \rightarrow 2r$. The violation of the local realistic bound occurs now for $r \sim 1$ and the entire Bell-CHSH function shown in Fig. 2 is "shifted back" on the r axis accordingly. This effect is the same when Eqs. (7) are used, although the form of C_{ef} is too cumbersome to be shown here. For clarity, we note that a two-mode squeezed state of squeezing r can be generated using two single-mode squeezed states of the same degree of squeezing and a beam splitter as

$$\hat{S}_{AB}(r)|00\rangle_{AB} = \hat{B}_{AB}\left(\frac{\pi}{2}\right)\hat{S}_A(r)\hat{S}_B(-r)|0,0\rangle_{AB}. \quad (16)$$

This means that single-mode squeezed states of $|r| \gtrsim 1$ ($\gtrsim 8.7$ dB) can be used as resources to show violations of Bell's inequality. This makes our proposal closer to an experimental implementation as such high levels of squeezing can be generated (for example, up to 10 dB [28]) using current technology. On the other hand, the local nonlinear operations may be more demanding and various types of unitary interactions need to be investigated to improve experimental feasibility of our approach.

V. CONCLUSIONS

We have shown a way to unveil violations of Bell's inequality for two-mode Gaussian states by means of nonlinear

local operations and Gaussian homodyne measurements. Besides its theoretical interest, which stays at the center of current investigations on entangled CV systems and their fundamental features, our study emerges as an appealing alternative to the current strategy for Bell's inequality tests based on the use of appropriately de-Gaussified resources and high-efficiency homodyning. Our proposal has been shown to be robust against the inefficiency of the homodyne detection and mixedness in the initial resource. This robustness is consistent with a previous study using entangled thermal states [16].

While the squeezing degree of $r \gtrsim 1$ required for resource Gaussian states is possible to achieve using present day technology, the strong nonlinear interactions required to implement the local operations may be more difficult to realize. On the other hand, it is worth noting that there has been remarkable progress to obtain strong nonlinear effects [21,29].

There remains some interesting future work. As the local operations used in our paper are not necessarily optimized ones, the research for more efficient local operations is desirable. Since we have used nonlinear operations to reveal violations of Bell's inequality for Gaussian states and Gaussian measurements, it is also natural to extend this investigation to entanglement distillation protocols for the Gaussian states. Interesting open questions are therefore whether there exist such entanglement distillation protocols using the type of local operations employed in this paper and how much they would be feasible and useful.

ACKNOWLEDGMENTS

M.P. thanks M. S. Kim for useful discussions and acknowledges the UK EPSRC for financial support (Grant No. EP/G004579/1). This work was supported by the Australian Research Council, Defence Science and Technology Organization, and the Korea Science and Engineering Foundation (KOSEF) grant funded by the Korean government (MEST) (Grant No. R11-2008-095-01000-0).

-
- [1] J. S. Bell, *Physics* (Long Island City, N.Y.) **1**, 195 (1964).
 [2] J. S. Bell, *Speakable and Unsayable in Quantum Mechanics* (Cambridge University Press, Cambridge, 1987).
 [3] A. Einstein, B. Podolsky, and N. Rosen, *Phys. Rev.* **47**, 777 (1935).
 [4] D. Bohm, *Quantum Theory* (Dover, New York, 1989).
 [5] L. Vaidman, *Phys. Rev. A* **49**, 1473 (1994); S. L. Braunstein and H. J. Kimble, *Phys. Rev. Lett.* **80**, 869 (1998); A. Furusawa *et al.*, *Science* **282**, 706 (1998); W. P. Bowen, N. Treps, B. C. Buchler, R. Schnabel, T. C. Ralph, Hans-A. Bachor, T. Symul, and P. K. Lam, *Phys. Rev. A* **67**, 032302 (2003); N. Takei, H. Yonezawa, T. Aoki, and A. Furusawa, *Phys. Rev. Lett.* **94**, 220502 (2005).
 [6] K. Banaszek and K. Wódkiewicz, *Phys. Rev. A* **58**, 4345 (1998).
 [7] T. C. Ralph, W. J. Munro, and R. E. S. Polkinghorne, *Phys. Rev. Lett.* **85**, 2035 (2000).
 [8] A. Gilchrist, P. Deuar, and M. D. Reid, *Phys. Rev. Lett.* **80**, 3169 (1998); W. J. Munro, *Phys. Rev. A* **59**, 4197 (1999); R. García-Patrón, J. Fiurášek, N. J. Cerf, J. Wenger, R. Tualle-Brouri, and Ph. Grangier, *Phys. Rev. Lett.* **93**, 130409 (2004).
 [9] H. Nha and H. J. Carmichael, *Phys. Rev. Lett.* **93**, 020401 (2004); R. Garcia-Patron, J. Fiurášek, N. J. Cerf, J. Wenger, R. Tualle-Brouri, and Ph. Grangier, *ibid.* **93**, 130409 (2004).
 [10] J. Fiurášek, *Phys. Rev. Lett.* **89**, 137904 (2002); J. Eisert, S. Scheel, and M. B. Plenio, *ibid.* **89**, 137903 (2002); G. Giedke and J. I. Cirac, *Phys. Rev. A* **66**, 032316 (2002).
 [11] H.-J. Briegel, W. Dür, J. I. Cirac, and P. Zoller, *Phys. Rev. Lett.* **81**, 5932 (1998).
 [12] J. F. Clauser, M. A. Horne, A. Shimony, and R. A. Holt, *Phys. Rev. Lett.* **23**, 880 (1969).
 [13] M. Stobińska, H. Jeong, and T. C. Ralph, *Phys. Rev. A* **75**,

- 052105 (2007).
- [14] H. Jeong and M. S. Kim, Phys. Rev. A **65**, 042305 (2002).
- [15] T. C. Ralph, A. Gilchrist, G. J. Milburn, W. J. Munro, and S. Glancy, Phys. Rev. A **68**, 042319 (2003).
- [16] H. Jeong, M. Paternostro, and T. C. Ralph, e-print arXiv:/0806.3558.
- [17] H. Jeong and T. C. Ralph, Phys. Rev. Lett. **97**, 100401 (2006); Phys. Rev. A **76**, 042103 (2007).
- [18] S. M. Barnett and P. M. Radmore, *Methods in Theoretical Quantum Optics* (Clarendon, Oxford, 1997).
- [19] J. Janszky and An. V. Vinogradov, Phys. Rev. Lett. **64**, 2771 (1990); V. Bužek, A. Vidiella-Barranco, and P. L. Knight, Phys. Rev. A **45**, 6570 (1992).
- [20] H. Jeong, M. S. Kim, T. C. Ralph, and B. S. Ham, Phys. Rev. A **70**, 061801 (2004).
- [21] M. Paternostro, M. S. Kim, and B. S. Ham, Phys. Rev. A **67**, 023811 (2003); J. Mod. Opt. **50**, 2565 (2003); V. S. Ilchenko, A. A. Savchenkov, A. B. Matsko, and L. Maleki, Phys. Rev. Lett. **92**, 043903 (2004).
- [22] B. S. Tsirelson, Lett. Math. Phys. **4**, 93 (1980).
- [23] For simplicity of presentation, the detection efficiencies are taken to be equal for both the homodyners, an assumption that can be easily relaxed.
- [24] M. S. Kim, W. Son, V. Buzek, and P. L. Knight, Phys. Rev. A **65**, 032323 (2002).
- [25] W. P. Bowen, P. K. Lam, and T. C. Ralph, J. Mod. Opt. **50**, 801 (2003).
- [26] G. J. Milburn, J. Phys. A **17**, 737 (1984); C. M. Caves and B. L. Schumaker, Phys. Rev. A **31**, 3068 (1985); R. Loudon and P. L. Knight, J. Mod. Opt. **34**, 709 (1987).
- [27] H. Jeong, J. Lee, and M. S. Kim, Phys. Rev. A **61**, 052101 (2000).
- [28] H. Vahlbruch, M. Mehmet, S. Chelkowski, B. Hage, A. Franzen, N. Lastzka, S. Goßler, K. Danzmann, and R. Schnabel, Phys. Rev. Lett. **100**, 033602 (2008).
- [29] M. Fleischhauer, A. Imamoğlu, and J. P. Marangos, Rev. Mod. Phys. **77**, 633 (2005); A. Imamoğlu, H. Schmidt, G. Woods, and M. Deutsch, Phys. Rev. Lett. **79**, 1467 (1997); H. Schmidt and A. Imamoğlu, Opt. Lett. **21**, 1936 (1996); L. V. Hau, S. E. Harris, Z. Dutton, and C. H. Behroozi, Nature (London) **397**, 594 (1999); Z.-B. Wang, K.-P. Marzlin, and B. C. Sanders, Phys. Rev. Lett. **97**, 063901 (2006); P. Bermel, A. Rodriguez, J. D. Joannopoulos, and M. Soljačić, *ibid.* **99**, 053601 (2007); F. G. S. L. Brandão, M. J. Hartmann, and M. B. Plenio, New J. Phys. **10**, 043010 (2008).